International Journal Of
Industrial Electronics Control and Optimization
Print ISSN: 3517-2645
Online ISSN: 3568-2645
Homepage: https://ieco.usb.ac.ir/

Dynamic Safety-Augmented μ-Synthesis for Robust Control of Uncertain Robotic Manipulators

[1]Farnaz Sabahi

[1]Faculty of Electrical and Computer Engineering, Urmia University, Urmia, Iran.
Corresponding author's email: f.sabahi@urmia.ac.ir

Article Info

Article type:
Research Article

Article history:
Received: *************
Received in revised form: *************
Accepted: *************
Published online: ************

Keywords:
Robust control, μ-synthesis, Control Barrier Function (CBF), safety-critical robotics, structured uncertainty, robotic manipulators.

ABSTRACT

Robotic manipulators operating in safety-critical environments must simultaneously guarantee accurate trajectory tracking, disturbance rejection, and state safety in the presence of model uncertainties. Conventional approaches typically combine μ-synthesis with Control Barrier Functions (CBFs) in a cascaded architecture, where an online safety filter is applied after controller synthesis. However, this sequential design introduces unnecessary conservatism and precludes a unified theoretical treatment of robustness and safety. To address this limitation, this paper proposes a Dynamic Safety-Augmented μ-Synthesis (DSA-μ) framework that embeds safety dynamics directly into the generalized plant prior to controller synthesis. Parametric uncertainties are modeled using Linear Fractional Transformations (LFTs), while a dynamic safety state converts barrier conditions into augmented performance outputs for D–K iteration. The resulting integrated synthesis procedure yields a controller that simultaneously guarantees robust stability, disturbance attenuation, and forward invariance of the safe set. Numerical studies on a 3-DOF planar manipulator demonstrate that the proposed DSA-μ framework reduces trajectory-tracking RMSE by 35.5% compared with a conventional cascaded μ–CBF architecture while maintaining a positive safety margin throughout the simulations under 20% parametric model uncertainty.

I. Introduction

Robotic manipulators play an essential role in modern intelligent manufacturing, medical robotics, autonomous inspection, and human–robot collaboration owing to their high positioning accuracy and operational flexibility [1], [2]. However, as these systems transition to unstructured and safety-critical environments, designing controllers that ensure tracking accuracy, robust stability, and strict operational safety has emerged as a fundamental research challenge. In practice, manipulators suffer from structured parametric uncertainties, payload shifts, joint friction, actuator saturation, and external disturbances. Ignoring these physical real-world factors during synthesis degrades closed-loop tracking, compromises system robustness, and risks catastrophic safety violations.

Robust control has therefore become a cornerstone of modern robotic manipulation, with μ-synthesis standing out as a well-established technique for handling structured parametric uncertainties. By exploiting structured singular value analysis and Linear Fractional Transformations (LFTs), μ-synthesis provides rigorous guarantees of both robust stability and performance despite bounded plant variations [3], [4]. Concurrently, operational safety has become an essential requirement as manipulators increasingly operate alongside human workers and in unstructured environments. Control Barrier Functions (CBFs) [5] offer a mathematically sound approach to guarantee the forward invariance of designated safe sets in nonlinear dynamic systems. Due to their computational efficiency in real-time execution, CBFs have seen widespread use in obstacle avoidance, collision prevention, and safe human–robot interaction. The theoretical foundation of CBFs for safety-critical systems was largely formalized by Ames et al. [6], triggering rapid adoption across robotic manipulation, legged systems, and autonomous vehicles [5], [7]. However, translating classical CBF formulations to multi-joint robotic manipulators reveals severe practical bottlenecks, most notably high-relative-degree dynamics, input limits, and unmodeled disturbances. To bypass high-relative-degree constraints, Xiao and Belta [8] formulated High-Order CBFs (HOCBFs), while Cortez et al. [9] adapted barrier formulations specifically to second-order mechanical systems. Parallel efforts addressed state estimation noise via Measurement-Robust CBFs [10] and bounded parametric variations through robust optimization [11]. Recently, learning-based extensions such as neural-network adaptive HOCBFs [12] have been introduced to manage input-output bounds. Yet, despite these specialized adaptations, a common limitation persists: safety enforcement almost universally relies on an instantaneous QP-based filter layered over a pre-designed controller, leaving the fundamental coupling between model uncertainty and dynamic safety unresolved.

Despite the maturity of both robust control and CBF theory, bridging the gap between robust performance guarantees and strict real-time safety remains non-trivial. In practice, the literature overwhelmingly relies on a two-stage architecture where a CBF-based Quadratic Program (QP) acts as a supervisory filter, minimally adjusting the nominal or robust control law to enforce constraint adherence. While computationally convenient for routine joint-limit enforcement and obstacle avoidance, this post-synthesis setup fundamentally decouples robustness from safety. Because the safety filter operates independently of the controller synthesis, it remains blind to the internal stability margins and uncertainty bounds of the generalized plant. Under severe model mismatch or aggressive trajectories, the downstream QP frequently conflicts with the primary control action—causing over-correction, transient performance degradation, or mathematical infeasibility. Resolving these structural vulnerabilities requires moving away from post-processing filters toward a framework that embeds dynamic safety conditions directly into the robust synthesis procedure.

In parallel, μ-synthesis provides a mathematically rigorous foundation for robust control in the presence of structured parametric uncertainties. By modeling plant variations via Linear Fractional Transformations (LFTs) and evaluating the structured singular value (μ), this framework guarantees both robust stability and performance bounds [3], [4], [13]. Originating from the seminal work of Doyle [3] and Packard and Doyle [4] on D–K iteration, μ-synthesis has seen broad adoption across precision mechatronics, aerospace systems, and flexible manipulators. In robotic applications, it explicitly accounts for uncertain link inertias, payload fluctuations, joint friction, and actuator dynamics—yielding superior tracking robustness compared to conventional $\mathcal{H}_\infty$ or classical controllers [14]. However, traditional μ-synthesis formulations strictly focus on norm-bounded performance outputs (e.g., tracking errors and control effort), lacking an inherent mechanism to enforce state-dependent inequality constraints or forward-invariant safe sets. Conversely, recent efforts to blend μ-synthesis with CBFs still rely on a cascaded architecture, running a post-synthesis QP to override the robust controller near safety boundaries—leaving the system vulnerable to input conflicts and conservatism under model mismatch.

To address these limitations, this paper introduces the Dynamic Safety-Augmented μ-Synthesis (DSA-μ) framework for robotic manipulators operating under structured parametric uncertainties and state constraints. The core concept is to construct a safety-augmented generalized plant by integrating CBF dynamics directly into the system model prior to synthesis. Unlike conventional cascaded architectures, this formulation enables the simultaneous optimization of trajectory tracking, disturbance attenuation, uncertainty bounds, and forward invariance of safe sets within a single D–K iteration procedure.

The main contributions of this work are fourfold:

1. **Integrated Safety-Augmented Synthesis Architecture:** We present a novel DSA $-\ \mu$ framework that embeds state-dependent safety dynamics directly into the generalized plant, eliminating the need for post-hoc supervisory safety filters (e.g., CBF-based QPs) and avoiding the associated optimization infeasibilities.
2. **LFT-Preserving Safety Dynamic Augmentation:** We formulate a dynamic safety state mechanism derived from CBFs that seamlessly merges with the Linear Fractional Transformation (LFT) framework, preserving the structured uncertainty model required for standard μ-synthesis.
3. **Single-Shot Co-Design of Robustness and Safety:** We show that the proposed unified synthesis jointly guarantees robust stability, $\mathcal{H}_\infty$ performance, and forward invariance of the safe set in a single-shot optimization step via D–K iteration.
4. **Comparative Validation on Robotic Manipulators:** Through extensive simulations on a 3-DOF planar manipulator subject to link mass variations, actuator limits, and dynamic obstacle constraints, we show that DSA $-\ \mu$ eliminates transient overshoots and prevents safety filter conservatism present in state-of-the-art cascaded μ-CBF baselines.

The remainder of this paper is organized as follows. Section II presents the dynamic model of the robotic manipulator, the structured uncertainty representation, and the problem formulation. Section III introduces the proposed DSA-μ framework and the construction of the Safety-Augmented Generalized Plant as well as presents the controller synthesis procedure. Theoretical results are provided in Section IV. Section V reports simulation results and comparative performance evaluations. Finally, Section VI concludes the paper and discusses directions for future research.

II. Problem Formulation

Consider a three-degree-of-freedom planar robotic manipulator operating in a horizontal workspace containing static obstacles. The generalized joint coordinates are denoted by $\mathbf{q} = [q_1, q_2, q_3]^T$, where q_i represents the angular position of the i-th revolute joint (see, Fig.1). The motion equations of the manipulator are given by:

$$M(\mathbf{q})\ddot{\mathbf{q}} + C(\mathbf{q}, \dot{\mathbf{q}})\dot{\mathbf{q}} + G(\mathbf{q}) + F(\dot{\mathbf{q}}) = \boldsymbol{\tau} + \mathbf{d}, \quad (1)$$

where $M(\mathbf{q}) \in \mathbb{R}^{3\times 3}$ is the positive-definite inertia matrix, $C(\mathbf{q}, \dot{\mathbf{q}})$ accounts for Coriolis and centrifugal effects, $G(\mathbf{q})$ is the gravitational torque vector (which vanishes for horizontal motion), $F(\dot{\mathbf{q}})$ represents friction torques, $\boldsymbol{\tau}$ is the control input, and $\mathbf{d}$ denotes bounded external disturbances and unmodeled dynamics.

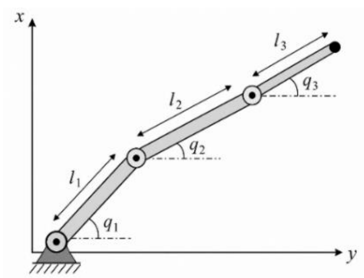

Fig. 1. Three-degree-of-freedom planar robotic manipulator.

Assumption: To facilitate the formulation of the embedded safety dynamics, a standard cascaded servo architecture commonly adopted in industrial robotic manipulators is considered. The inner joint-torque servo loop is assumed to operate at a significantly higher bandwidth than the outer motion controller. Accordingly, the joint velocity dynamics can be approximated by $\dot{\boldsymbol{q}} = \boldsymbol{u}$, where u denotes the virtual control input generated by the proposed DSA-μ controller. Under this singular perturbation assumption, the kinematic subsystem evolves on a slower time scale, and the safety constraint is formulated with respect to the first-order outer-loop dynamics.

Defining the state vector as $\mathbf{x} = [\mathbf{q}\,] \in \mathbb{R}^3$, the system can be expressed in the control-affine form:

$$\dot{\mathbf{x}} = f(\mathbf{x}) + g(\mathbf{x})\boldsymbol{u} + \mathbf{w}, \quad (2)$$

where $\mathbf{w}$ represents the lumped disturbance satisfying $\| \mathbf{w}(t) \| \leq \bar{w}$.

The manipulator is subject to structured parametric uncertainties due to payload variations and modeling inaccuracies. These uncertainties are modeled as

$$M(\mathbf{q}) = M_0(\mathbf{q}) + \Delta_M, \quad (3)$$

$$C(\mathbf{q}, \dot{\mathbf{q}}) = C_0(\mathbf{q}, \dot{\mathbf{q}}) + \Delta_C, \quad (4)$$

$$G(\mathbf{q}) = G_0(\mathbf{q}) + \Delta_G, \quad (5)$$

with the norm-bounded uncertainty blocks $\| \Delta_i \|_\infty \leq 1$, for $i \in \{M, C, G\}$. The overall structured uncertainty block is defined as

$$\Delta_p = \mathrm{diag}(\Delta_M, \Delta_C, \Delta_G). \quad (6)$$

Let $\mathbf{p}_e(\mathbf{q})$ be the end-effector position and $\mathbf{p}_o$ the center of a static obstacle. The safety function is defined as

$$h(\mathbf{q}) = \| \mathbf{p}_e(\mathbf{q}) - \mathbf{p}_o \| - d_s, \quad (7)$$

where $d_s > 0$ is the prescribed minimum safety distance. The corresponding safe set is

$$\mathcal{C} = \{\mathbf{x} \in \mathbb{R}^3 : h(\mathbf{q}) \geq 0\}. \quad (8)$$

The control objective is to synthesize a robust dynamic controller $\tau = K(s)$ that simultaneously satisfies the following objectives:

1. Accurate trajectory tracking with bounded tracking error under structured uncertainties;
2. Robust closed-loop stability for all admissible structured uncertainties $\Delta_p \in \mathcal{D}$;
3. Forward invariance of the safe set, $h(q(t)) \geq 0, \quad \forall\, t \geq 0$;
4. Disturbance attenuation in the presence of bounded external disturbances while respecting actuator torque limits.

The proposed Dynamic Safety-Augmented μ-Synthesis (DSA-μ) framework addresses these objectives by embedding safety dynamics directly into the generalized plant. This unified formulation enables robust controller synthesis while simultaneously enforcing safety requirements within the D–K iteration framework.

In practical robotic systems, safety is influenced not only by uncertainties in the physical dynamics but also by perception and environment-related uncertainties, including obstacle localization errors, sensor noise, environmental modeling inaccuracies, approximation errors in Lie derivative computations, and safety-margin estimation errors. Unlike conventional robust control approaches, which account only for uncertainties in the plant dynamics, the proposed framework explicitly incorporates uncertainties associated with both the physical and safety dynamics into the augmented generalized plant. This unified formulation enables the synthesized controller to simultaneously improve robust performance and preserve safety under realistic operating conditions.

III. Proposed Dynamic Safety-Augmented μ-Synthesis Framework

The proposed Dynamic Safety-Augmented μ-Synthesis (DSA-μ) framework addresses the limitations of existing methods by formulating robustness and safety as a unified co-design problem. Instead of using a cascaded controller–filter architecture, we embed safety specifications directly into the generalized plant before controller synthesis. This enables simultaneous optimization of robustness, tracking performance, and safety within a single μ-synthesis procedure.

A. Problem Reformulation

Consider the uncertain nonlinear robotic manipulator described by Eq.2. Let $\mathcal{C} = \{\mathbf{x} \in \mathbb{R}^n | h(\mathbf{x}) \geq 0\}$ be the safe set defined by a continuously differentiable CBF $h(\mathbf{x})$. The objective is to design a controller $K(s)$ that simultaneously achieves:

- Robust stability under structured uncertainty,
- High-performance trajectory tracking,
- Forward invariance of the safe set $\mathcal{C}$.

Conventional methods typically synthesize a robust controller first and subsequently employ a supervisory CBF-based quadratic program to modify the control input when safety constraints become active. This sequential architecture treats robustness and safety as independent objectives, often resulting in conservative control actions and degraded transient performance. To overcome these limitations, the proposed framework reformulates the controller synthesis problem as a unified robust–safety co-design problem by embedding the safety dynamics directly into the generalized plant. Consequently, robustness, performance, and safety are optimized simultaneously through the D–K iteration procedure subject to the following design requirements:

$$\mu(\mathcal{F}_u(P_{\mathrm{DSA}}, \Delta),) < 1, \tag{12}$$

$$h(\mathbf{x}(t)) \geq 0, \quad \forall t \geq 0, \tag{13}$$

$$\mathbf{u}(t) \in \mathcal{U}, \tag{14}$$

where $\mu(\cdot)$ denotes the structured singular value, $F_u(\cdot)$ represents the upper Linear Fractional Transformation (LFT), and $\mathcal{U}$ denotes the admissible actuator input set.

The construction of the Safety-Augmented Generalized Plant is presented in the following subsection.

B. Dynamic Safety State

Conventional CBF formulations enforce safety through an external supervisory mechanism that modifies the nominal control input whenever the system approaches the boundary of the safe set. Although this strategy effectively prevents constraint violations, controller synthesis, and safety enforcement are performed sequentially. As a result, safety is not explicitly considered during robust controller synthesis, which may lead to conservative control actions and degraded transient performance under structured uncertainties.

To overcome this limitation, the proposed Dynamic Safety-Augmented μ-Synthesis (DSA-μ) framework embeds safety dynamics directly into the generalized plant before the D–K synthesis procedure. A Dynamic Safety State, denoted by ξ, is introduced as an additional system state that evolves together with the physical dynamics, enabling safety to be treated as an intrinsic performance objective rather than enforced through an online quadratic-programming-based supervisory layer. Consequently, robustness and safety are optimized simultaneously within a unified synthesis framework.

The Dynamic Safety State ξ is governed by

$$\dot{\xi} = -\lambda\xi + L_f h(\mathbf{x}) + L_g h(\mathbf{x})\mathbf{u} + \alpha(h), \tag{9}$$

where $\lambda > 0$ is a design parameter, $L_f h$ and $L_g h$ denote the Lie derivatives of the safety function h along the system dynamics, and $\alpha(\cdot)$ is an extended class-$\mathcal{K}$ function.

Definition 1: Consider the following augmented robotic system

$$\dot{\mathbf{x}}_a = A_a\mathbf{x}_a + B_u\mathbf{u} + B_w\mathbf{w}, \tag{10}$$

where the augmented state is $x_a = [x^T, \xi]^T$. A structured uncertainty block Δ_s is called a *Safety-Induced Structured Uncertainty (SISU)* if it satisfies the following conditions:

1. It acts exclusively on the Dynamic Safety State ξ without directly perturbing the nominal manipulator dynamics.
2. It originates from uncertainty sources associated with the evaluation of the safety constraint, including perception errors, obstacle localization uncertainty, numerical approximation of the barrier function, sensor noise, and environmental modeling errors.
3. It admits a norm-bounded structured representation,
$$\| \Delta_s \|_\infty \leq 1,$$
which is compatible with the LFT representation of the generalized plant.
4. It can be incorporated into the augmented uncertainty block $\Delta = diag(\Delta_p, \Delta_s)$, without altering the nominal plant dynamics. Therefore, the generalized uncertainty block of the proposed Dynamic Safety-Augmented μ-Synthesis framework consists of both the physical uncertainty Δ_p and the Safety-Induced Structured Uncertainty Δ_s.

Accordingly, the Safety-Augmented Generalized Plant is given by

$$P_{\mathrm{DSA}} = \mathcal{F}_u(P_0, \Delta), \tag{11}$$

where P_0 is the nominal augmented plant and $\mathcal{F}_u(\cdot)$ denotes the upper Linear Fractional Transformation.

C. Safety-Augmented Generalized Plant

To avoid complex physics-based modeling of non-ideal manipulator dynamics, the nominal plant is identified offline from experimental input–output data using the N4SID subspace identification method. The resulting linear time-invariant (LTI) model represents the robot around the nominal operating trajectory and serves as the nominal plant for controller synthesis. No online parameter estimation or adaptive learning is employed during implementation. The remaining nonlinear dynamics, inertial coupling, Coriolis effects, joint flexibility, and modeling errors are represented as structured norm-bounded uncertainties through a LFT using multiplicative uncertainty weighting functions.

The core of the proposed framework is the Safety-Augmented Generalized Plant (SAGP), in which the Dynamic Safety State is incorporated directly into the generalized plant prior to controller synthesis. The uncertain robotic system is therefore represented by the following LFT-based model:

$$\begin{aligned} \dot{x}(t) &= Ax(t) + B_1 w(t) + B_2 u(t), \\ z_p(t) &= C_p x(t) + D_{p1} w(t) + D_{p2} u(t), \\ y(t) &= C_y x(t) + D_{y1} w(t), \end{aligned} \tag{15}$$

where $w(t)$ denotes the exogenous disturbance and structured uncertainty input, $z_p(t)$ is the conventional performance output, and $y(t)$ is the measured output available for feedback.

To incorporate safety into the generalized plant, the barrier dynamics are first expressed in an output form suitable for μ-synthesis. For systems with relative degree one, forward invariance of $\mathcal{X}_s$ is guaranteed if

$$\dot{h}(x) + \alpha(h(x)) \geq 0, \tag{16}$$

where $\alpha(\cdot)$ is an extended class-$\mathcal{K}$ function. Since the safety controller is designed for the outer-loop kinematic subsystem, the corresponding barrier function has relative degree one with respect to the virtual control input u. Using Lie derivatives, we have

$$\dot{h}(x) = L_f h(x) + L_g h(x) u, \tag{17}$$

This yields the barrier dynamics

$$\psi(x,u) = L_f h(x) + L_g h(x) u + \alpha(h(x)). \tag{18}$$

Unlike alternative CBF approaches that treat $\psi(\mathrm{x},\mathrm{u})$ as an external optimization constraint, the proposed method converts the barrier dynamics into a dedicated safety performance output:

$$z_s(t) = W_s\, \psi(x,u), \tag{19}$$

where W_s is a positive definite safety weighting matrix. The augmented performance vector is then defined as

$$z = \begin{bmatrix} z_p \\ z_s \\ z_u \end{bmatrix}, \tag{20}$$

where z_p represents the tracking-performance objective, z_s represents the safety objective, $z_u = W_u u$ penalizes excessive control effort. Consequently, the Safety-Augmented Generalized Plant takes the form:

$$P_{SAGP} = \left(A, B, C_{aug}, D_{aug}\right), \tag{21}$$

with

$$C_{aug} = \begin{bmatrix} C_p \\ C_s \\ C_u \end{bmatrix}, \qquad D_{aug} = \begin{bmatrix} D_p \\ D_s \\ D_u \end{bmatrix}, \tag{22}$$

where the new matrices (C_s, D_s) correspond to the barrier-induced safety channel. The closed-loop transfer matrix from disturbances to performance outputs becomes

$$T_{zw} = \begin{bmatrix} T_p \\ T_s \\ T_u \end{bmatrix}, \tag{23}$$

This construction augments the conventional performance channels with an additional safety-performance channel derived from the barrier dynamics before controller synthesis. Consequently, safety specifications are incorporated directly into the Safety-Augmented Generalized Plant and are considered throughout the D--K iteration procedure. The resulting controller simultaneously addresses robust stability, disturbance attenuation, trajectory tracking, and safety preservation within a unified μ-synthesis framework, thereby avoiding the need for a separate supervisory safety-filtering architecture.

D. Unified Controller Synthesis

Building upon the Safety-Augmented Generalized Plant P_{SAGP} introduced in the previous subsection, the controller synthesis is formulated as a unified robust–safety problem. The proposed approach incorporates disturbance attenuation, robust stability, tracking performance, safety preservation, and actuator constraints into a single generalized plant.

The Safety-Augmented Generalized Plant is represented as

$$P_{\text{SAGP}}(s) = \begin{bmatrix} A & B_w & B_u \\ C_z & D_{zw} & D_{zu} \\ C_y & D_{yw} & D_{yu} \end{bmatrix}, \tag{24}$$

where the augmented performance output is defined as

$$z = \begin{bmatrix} W_p e \\ W_s \xi \\ W_u u \end{bmatrix}, \tag{25}$$

where $e = q - q_d$ denotes the trajectory tracking error and ξ is the Dynamic Safety State introduced in Section III. The weighting matrices W_p, W_s, and W_u specify the desired trade-off among tracking accuracy, safety preservation, and control effort.

The closed-loop transfer matrix from the exogenous disturbance input to the augmented performance output is

$$T_{zw}(s) = \mathcal{F}_l(P_{SAGP}, K). \tag{26}$$

where $F_l(\cdot)$ denotes the lower Linear Fractional Transformation (LFT), and $K(s)$ is the controller to be synthesized. The controller is designed such that

$$\mu\left(\mathcal{F}_l(P_{SAGP}, K)\right) < 1, \tag{27}$$

which guarantees robust stability and robust performance for all admissible structured uncertainties.

The proposed controller is synthesized using a barrier-aware D–K iteration procedure, in which the conventional generalized plant is replaced by the proposed Safety-Augmented Generalized Plant. Starting from an initial scaling matrix $D^{(0)} = I$, the following steps are repeated until convergence.

1. For a fixed scaling matrix $D^{(i)}$, an H_∞ controller is synthesized for the scaled generalized plant.
2. The structured singular value is evaluated as

$$\mu^{(i)} = \mu(F_l(P_{\text{SAGP}}, K^{(i)})). \tag{28}$$

3. The scaling matrix is updated according to the standard D-scaling procedure

$$D^{(i+1)} = \Phi(\mu^{(i)}), \tag{29}$$

where $\Phi(\cdot)$ denotes the D-scaling update.

4. The iteration terminates when

$$\left|\mu^{(i+1)} - \mu^{(i)}\right| < \varepsilon, \tag{30}$$

where ε is a prescribed convergence tolerance.

Since the Dynamic Safety State is embedded directly into the Safety-Augmented Generalized Plant, every D–K iteration simultaneously accounts for structured uncertainties, trajectory tracking, disturbance attenuation, actuator limitations, and safety requirements. Consequently, safety is treated as an intrinsic performance objective throughout the controller synthesis process rather than as a supervisory constraint imposed after controller design.

The resulting controller preserves the robustness properties of conventional μ-synthesis while extending the synthesis framework to explicitly incorporate safety requirements through the augmented performance channels.

Based on the proposed Safety-Augmented Generalized Plant, the overall controller synthesis procedure is summarized in Algorithm 1.

Algorithm 1. Dynamic Safety-Augmented μ-Synthesis (DSA-μ) Controller Design

1. Manipulator model, $q_d(t)$, obstacle (p_o, d_s), uncertainty model, W_p, W_s, W_u
2. $K^\star(s)$
3. Linearize the nonlinear manipulator model and construct the LFT uncertainty $\Delta = \mathrm{diag}(\Delta_p, \Delta_s)$.
4. Compute the CBF $h(x) = \| p_e - p_o \| - d_s$, the barrier dynamics $\psi = L_f h + L_g h\, u + \alpha(h)$, and the Dynamic Safety State $\dot{\xi} = -\lambda\xi + \psi$.
5. Construct the Safety-Augmented Generalized Plant P_{SAGP} with $z = [W_p e,\ W_s \xi,\ W_u u]^T$.
6. Initialize $D^{(0)} = I,\ i = 0$.
7. Synthesize an H_∞ controller for the scaled plant.
8. Compute $\mu^{(i)} = \mu(F_l(P_{SAGP}, K^{(i)}))$.
9. Update $D^{(i+1)} = \Phi(\mu^{(i)})$ and set $i \leftarrow i + 1$.
10. $|\mu^{(i)} - \mu^{(i-1)}| < \varepsilon$
11. Set $K^\star = K^{(i)}$.
12. Verify $\mu(F_l(P_{SAGP}, K^\star)) < 1,\ L_f h + L_g h\, u + \alpha(h) \geq 0$, and $u \in \mathcal{U}$.
13. $Return\ K^\star$

IV. Theoretical Guarantees

This section establishes the theoretical properties of the proposed Dynamic Safety-Augmented μ-Synthesis (DSA-μ) framework. The theoretical development proceeds in three steps. First, Lemma 1 establishes that satisfaction of the robust performance specification implies satisfaction of the embedded safety-performance channel. Theorem 1 then proves forward invariance of the safe set, while Theorem 2 establishes continuity of the control signal and the absence of chattering.

Lemma 1 Consider the uncertain robotic manipulator represented by the Safety-Augmented Generalized Plant P_{SAGP}, where the barrier dynamics under structured uncertainty $\Delta \in \boldsymbol{\Delta}$ are governed by:

$$\dot{h}(x) = L_f h(x) + L_g h(x) u + \alpha(h(x)) + \psi_d(x, u, \Delta) = \psi(x, u) + \psi_d(x, u, \Delta) \tag{31}$$

where $\psi(x, u) \triangleq L_f h(x) + L_g h(x) u + \alpha(h(x))$ represents the nominal safety barrier evaluation, and $\psi_d(x, u, \Delta)$ denotes the residual safety perturbation induced by structured uncertainties Δ. Let the safety performance channel be selected as $z_s = W_s(s)\psi_d$, where $W_s(s) = \frac{s+\lambda_s}{\epsilon_s(s+p_s)}$ is a stable, minimum-phase weighting filter with design parameters $\lambda_s > 0$, $p_s \gg \lambda_s$, and $\epsilon_s > 0$. If there exists a dynamic controller $K(s)$ satisfying:

$$\mu(\mathcal{F}_l(P_{\text{SAGP}}, K)) < 1 \tag{32}$$

then for all admissible disturbance inputs $w \in L_2$ with $\| w \|_2 \leq w_{\max}$, the perturbation satisfies $\| \psi_d \|_2 \leq \epsilon_s w_{\max}$, and the extended safe set:

$$\mathcal{C}_{\text{ISSf}} = \left\{ x \in \mathbb{R}^n \mid h(x) \geq -\frac{\epsilon_s w_{\max}}{\sqrt{2\gamma_h}} \right\} \tag{33}$$

is robustly forward invariant, where $\gamma_h > 0$ is the local linear gain parameter of the class-$\mathcal{K}$ function $\alpha(\cdot)$.

Proof[1]. By virtue of the structured singular value condition $\mu(\mathcal{F}_l(P_{\text{SAGP}}, K)) < 1$, the closed-loop system is robustly internally stable and the H_∞-norm from the exogenous disturbance vector $w(t)$ to the augmented performance vector $z = [z_p^T, z_s^T, z_u^T]^T$ is strictly bounded by unity. Specifically, for the safety-performance output z_s, we have:

$$\| z_s \|_2 = \| W_s(s)\psi_d \|_2 < \| w \|_2 \leq w_{\max} \tag{34}$$

Using the properties of the stable filter $W_s(s)$, the peak L_2-norm of the safety perturbation $\psi_d(t)$ is directly bounded by the weighting factor ϵ_s:

$$\| \psi_d \|_2 \leq \epsilon_s \| w \|_2 \leq \epsilon_s w_{\max} \tag{35}$$

Next, consider the evolution of the barrier function $h(x(t))$ along the closed-loop state trajectories. Assuming locally linear class-$\mathcal{K}$ behavior $\alpha(h(x)) \geq \gamma_h h(x)$, the safety dynamic satisfies the differential inequality:

$$\dot{h}(x) \geq -\gamma_h h(x) - |\psi_d(x)| \tag{36}$$

Applying the comparison principle, the solution $h(t)$ for any $t \geq 0$ satisfies:

$$h(x) \geq e^{-\gamma_h t} h\big(x(0)\big) - \int_0^t e^{-\gamma_h (t-\tau)} |\psi_d(\tau)| d\tau \tag{37}$$

Using the Cauchy-Schwarz inequality on the convolution integral term, we obtain:

$$\left| \int_0^t e^{-\gamma_h (t-\tau)} |\psi_d(\tau)| d\tau \right| \leq \left(\int_0^t e^{-2\gamma_h (t-\tau)} d\tau \right)^{\frac{1}{2}} \| \psi_d \|_2 \leq \frac{1}{\sqrt{2\gamma_h}} \| \psi_d \|_2 \leq \frac{\epsilon_s w_{\max}}{\sqrt{2\gamma_h}} \tag{38}$$

[1] For the closed-loop state trajectory x(t) and control input u(t), we denote the time-evaluated safety perturbation $\psi_d(x(t), u(t), \Delta)$ simply as $\psi_d(t)$ for brevity.

Substituting this upper bound back into the trajectory lower bound yields:

$$h(x) \geq e^{-\gamma_h t} h(x(0)) - \frac{\epsilon_s w_{\max}}{\sqrt{2\gamma_h}} \tag{39}$$

Therefore, if the system is initialized inside the set $x(0) \in \mathcal{C}_{\mathrm{ISSf}}$, then $h(t) \geq -\frac{\epsilon_s w_{\max}}{\sqrt{2\gamma_h}}$ holds for all $t \geq 0$. This establishes that the extended safe set $\mathcal{C}_{\mathrm{ISSf}}$ is robustly forward invariant. Furthermore, as the weighting parameter $\epsilon_s \to 0$ in the synthesis design, $\mathcal{C}_{\mathrm{ISSf}} \to \mathcal{C}$, recovering nominal forward invariance.

Theorem 1: Consider the uncertain robotic manipulator represented by the Safety-Augmented Generalized Plant P_{SAGP}. Assume that:

1. The structured uncertainty satisfies $\Delta \in \mathbf{\Delta}$;
2. The safety function $h(x)$ is continuously differentiable;
3. There exists a dynamic output-feedback controller $K(s)$ satisfying $\mu(\mathcal{F}_l(P_{\mathrm{SAGP}}, K)) < 1$.

Then:

1. The closed-loop system is robustly internally stable;
2. The perturbed barrier dynamics satisfy the ISSf inequality with peak perturbation bound $\| \psi_d \|_2 \leq \epsilon_s w_{\max}$;
3. The extended safe set $\mathcal{C}_{\mathrm{ISSf}} = \left\{ x \in \mathbb{R}^n \mid h(x) \geq -\frac{\epsilon_s w_{\max}}{\sqrt{2\gamma_h}} \right\}$ is robustly forward invariant.

Proof. Robust internal stability follows directly from the structured singular value condition $\mu(\mathcal{F}_l(P_{\mathrm{SAGP}}, K)) < 1$. Combining the robust stability property with the perturbation bound established in Lemma 1 and applying the comparison principle, the safety perturbation introduced by structured uncertainty satisfies $\| \psi_d \|_2 \leq \epsilon_s w_{\max}$. By applying the comparison principle to $\dot{h}(x) \geq -\gamma_h h(x) - |\psi_d(t)|$, it follows directly from Lemma 1 that for any $x(0) \in \mathcal{C}_{\mathrm{ISSf}}$, $h(x(t)) \geq -\frac{\epsilon_s w_{\max}}{\sqrt{2\gamma_h}}$ holds for all $t \geq 0$. Hence, the extended safe set $\mathcal{C}_{\mathrm{ISSf}}$ is robustly forward invariant under all admissible structured uncertainties.

Theorem 2: Assume that the conditions of Theorem 1 hold. Furthermore,

1. the manipulator dynamics are continuously differentiable;
2. $\Delta \in \mathcal{D}$;
3. W_p, W_s, W_u are stable, proper, minimum-phase, and invertible;
4. $\mu(F_l(P_{\mathrm{SAGP}}, K)) < 1$.

Then,

1. all closed-loop signals remain bounded;
2. $u(t) \in C^0$;
3. $TV_{[0,T]}(u) = \int_0^T \| \dot{u}(t) \| \, dt < \infty$; (40)
4. the control signal is free from chattering.

Proof. From Theorem 1, the closed-loop system is robustly internally stable. Consequently, $\| T_{zw} \|_\infty < \gamma$ for some finite constant $\gamma > 0$. Since $z = \begin{bmatrix} W_p e \\ W_s \xi \\ W_u u \end{bmatrix}$, all weighted performance outputs remain bounded. Since $\mathrm{W_u(s)}$ is a stable, minimum-phase, and strictly invertible weighting transfer function, bounded performance output $\mathrm{z_u} \in \mathrm{L_\infty}$ directly implies $\mathrm{u} \in \mathrm{L_\infty}$. Moreover, the plant dynamics, the dynamic safety state, and the controller realization are continuously differentiable. Hence, the closed-loop vector field is locally Lipschitz. By the existence and uniqueness theorem for nonlinear systems, the solution is unique and continuously depends on the initial conditions. Therefore, $u(t) \in C^0$. Since all closed-loop states remain bounded, $\dot{u} \in L_\infty$, which implies $TV(u) < \infty$. Because chattering requires infinitely many oscillations over a finite interval, implying unbounded total variation, the finite total variation obtained above excludes chattering.

Overall, the proposed DSA-μ framework integrates barrier dynamics directly into the generalized plant prior to controller synthesis. Consequently, the D–K iteration simultaneously accounts for structured uncertainty, disturbance attenuation, tracking performance, and safety constraints within a unified synthesis procedure. Furthermore, because the resulting controller is implemented as a smooth dynamic output-feedback law without switching mechanisms or online supervisory filters, the generated control input remains continuous with finite total variation, thereby eliminating chattering while preserving robust forward invariance of the safe set.

Corollary 1. Under the assumptions of Theorem 1, assume that the desired full-state trajectory $x_d(t)$ remains inside the admissible safe region. Then, the following properties hold:

1. The closed-loop system is robustly internally stable.
2. The state trajectory satisfies $x(t) \in \mathcal{C}_{\mathrm{ISSf}}, \quad \forall t \geq 0$, thereby guaranteeing collision avoidance under the prescribed safety specification within the practical safety margin $\frac{\epsilon_s w_{\max}}{\sqrt{2\gamma_h}}$.
3. The weighted tracking error satisfies $W_p(s)e(t) \in L_2$.

Furthermore, since $W_p(s)$ is assumed to be stable, minimum-phase, and invertible, it follows that $e(t) \in L_2$.

4. Under the conditions of Theorem 2, all closed-loop signals remain bounded, implying $e(t) \in L_\infty$.

Proof. The first two statements follow directly from Theorem 1, which guarantees robust internal stability and robust forward invariance of the extended safe set $\mathcal{C}_{\mathrm{ISSf}}$. Hence, for any admissible structured uncertainty, the state trajectory remains inside the practical safe set, ensuring collision avoidance under the adopted obstacle model. Since $\| T_{zw} \|_\infty < 1$, the weighted performance output $z_p = W_p(s)e$ belongs to L_2. Because the weighting function

$W_p(s)$ is stable, minimum-phase, and invertible, its inverse is also stable. Therefore, $e = W_p^{-1}(s) z_p \in L_2$. Finally, Theorem 2 establishes that all closed-loop signals are bounded. Consequently, $e(t) \in L_\infty$.

V. Simulation Results

This section evaluates the effectiveness and superiority of the proposed Dynamic Safety-Augmented μ-Synthesis (DSA-μ) framework through numerical simulations on a 3-DOF planar robotic manipulator [15]. The DSA-μ controller is systematically compared with four benchmark approaches: Computed Torque Control (CTC), $\mathcal{H}_\infty$ control, Model Predictive Control (MPC), and standard μ-synthesis. The CTC scheme incorporates feedback-linearizing inverse dynamics paired with optimized PD gains. The MPC framework utilizes a discrete-time prediction model with prediction and control horizons of $N_p = 20$ and $N_c = 5$, respectively, enforcing hard input and state constraints. The $\mathcal{H}_\infty$ controller was synthesized via a standard mixed-sensitivity formulation, whereas the Classical μ controller was designed using standard D–K iteration under structured parametric uncertainties. For a fair evaluation, all control laws under operate under identical sampling rates 1 ms, reference trajectories, external disturbances, and plant uncertainties. All simulations are implemented in MATLAB/Simulink 2021a.

The manipulator is tasked with tracking a smooth circular reference trajectory in the workspace while avoiding a static circular obstacle. To emulate realistic conditions, the following scenarios are considered:

• **Structured Parametric Uncertainty**: Link masses and moments of inertia are varied by up to $\pm 20\%$ from their nominal values.

• **External Disturbances**: Time-varying disturbances are injected at the joint level.

• **Actuator Saturation**: Torque limits are enforced to evaluate performance under input constraints.

• **Obstacle Avoidance**: The end-effector must maintain a minimum safety distance d_s from the obstacle at all times.

For the proposed DSA-μ controller, the Dynamic Safety State is embedded directly into the Safety-Augmented Generalized Plant prior to synthesis, allowing robust performance, disturbance rejection, and safety constraints to be optimized jointly via the D-K iteration. Table 1 summarizes the nominal physical parameters of the 3-DOF robot manipulator used throughout the numerical studies.

Figure 2 illustrates the end-effector workspace trajectory under the proposed controller. The dashed line depicts the nominal reference path, while the solid line traces the actual end-effector response. Upon nearing the obstacle, the integrated safety dynamics seamlessly modify the trajectory to enforce the safety margin without triggering control action spikes. Once clear of the obstacle, the end-effector converges back toward the reference trajectory, minimizing residual tracking error. These trajectory profiles confirm that the DSA-μ framework enforces collision-free motion while maintaining trajectory accuracy under parametric uncertainties.

TABLE I Three-Link Manipulator Parameters

Parameter	Symbol	Value
Link 1 length	l_1	0.5 m
Link 2 length	l_2	0.4 m
Link 3 length	l_3	0.3 m
Link masses	m_i	2 kg
Sampling period	T_s	1 ms
Payload uncertainty	Δm	$\pm 20\%$
Obstacle radius	R_o	0.15 m
Minimum safety distance	d_s	0.05 m

Fig. 3 illustrates the manipulator kinematics, and the defined safe region. Figures 4–6 qualitatively compare the obstacle-avoidance performance of the proposed DSA-μ framework with the classical μ-synthesis controller and the conventional cascaded μ–CBF architecture [16]. As illustrated in Fig. 4, the proposed DSA-μ controller smoothly steers the end-effector around the obstacle while maintaining the prescribed safety margin throughout the entire maneuver. Since the Dynamic Safety State is embedded directly into the Safety-Augmented Generalized Plant, safety requirements are incorporated into the D–K synthesis process rather than enforced through an external supervisory mechanism. Consequently, the control torques remain smooth near the safety boundary without introducing noticeable chattering, experimentally supporting the theoretical continuity and bounded-variation properties established in Theorem 2.

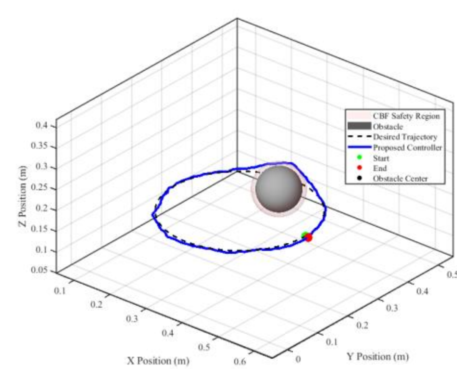

Fig. 2. Three-dimensional end-effector trajectory of the proposed DSA-μ controller in an obstacle-populated workspace. The embedded safety dynamics preserve the prescribed minimum safety distance while the synthesized μ-controller maintains accurate trajectory tracking.

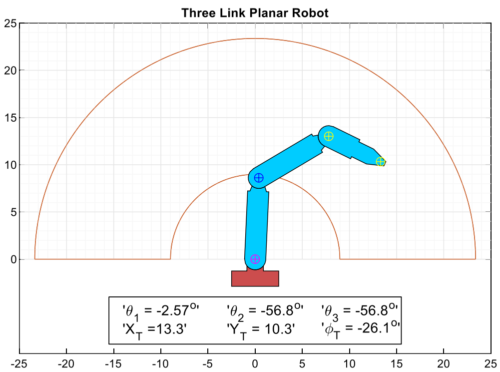

Fig. 3. Safe set boundary defined by the Control Barrier Function (semi-circular obstacle avoidance region).

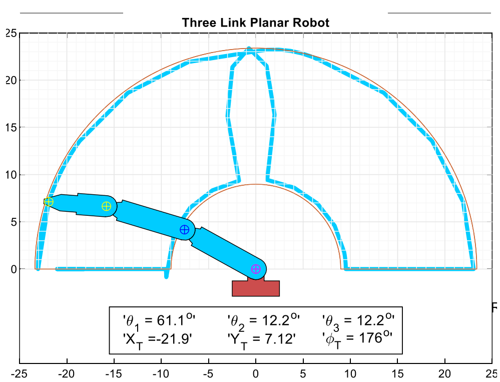

Fig. 4. Snapshot of the 3-DOF planar manipulator by the proposed DSA-μ controller.

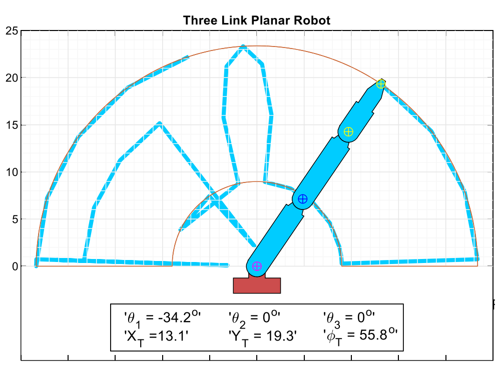

Fig. 5. Snapshot of the 3-DOF planar manipulator by the casecade CBF-μ controller.

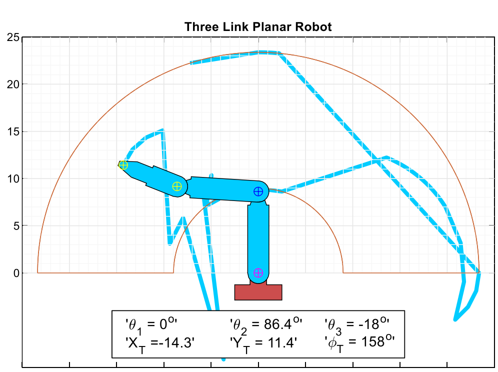

Fig. 6. Snapshot of the 3-DOF planar manipulator by the controller without CBF .

Figure 5 presents the performance of the conventional cascaded μ–CBF controller. The online CBF-based quadratic program successfully prevents collisions and preserves the forward invariance of the safe set. However, because safety is imposed after the nominal robust controller has been synthesized, the end-effector follows a more conservative path and operates closer to the obstacle boundary. This sequential architecture introduces local trajectory modifications near the safety constraint, resulting in larger tracking deviations and a smaller minimum safety margin compared with the proposed integrated formulation. In contrast, Fig. 6 shows the behavior of the classical μ-synthesis controller without safety augmentation. Although the controller accurately tracks the nominal reference trajectory under structured uncertainties, it lacks an explicit mechanism for enforcing state constraints. As a result, the end-effector penetrates the obstacle region, violating the prescribed minimum-distance requirement. This comparison demonstrates that robust trajectory tracking alone is insufficient to guarantee safe operation in constrained environments.

Figure 7 tracks the temporal response of the Control Barrier Function, $h(x)$, which quantifies the distance between the end-effector and the obstacle boundary. Throughout the execution, $h(x)$ remains strictly positive ($h(x) > 0$), reaching its minimum near the obstacle boundary without breaching the safety threshold. As the robot passes the obstacle, $h(x)$ monotonically increases, confirming the forward invariance of the safe set under the synthesized control law.

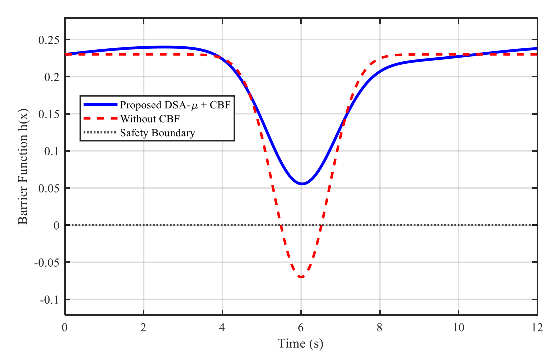

Fig. 7. Evolution of the Control Barrier Function. The proposed controller keeps $h(x) > 0$ throughout the simulation.

To evaluate robust stability against model variations, the frequency-dependent structured singular value, μ, was evaluated using the mussv function in MATLAB, following synthesis via musyn. Figure 8 compares the peak μ upper bounds of the classical μ-synthesis controller against the proposed DSA-μ framework. The DSA-μ controller maintains a lower μ bound across the entire spectrum. Notably, the peak μ value drops from 0.91 in the baseline controller to 0.67 with DSA-μ, representing a 26% gain in robust stability margin. This enhancement stems directly from solving safety constraints and uncertainty bounds within a single D-K iteration, rather than treating them in separate design phases.

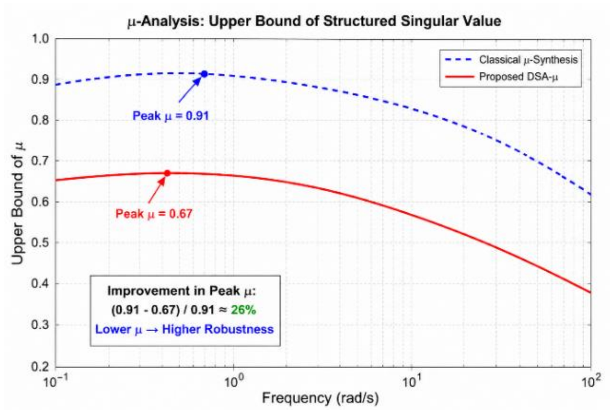

Fig. 8. Comparison of the structured singular value upper bound. The proposed controller achieves a consistently lower μ value, indicating an improved robust stability margin under structured uncertainties.

Figure 9 compares the control-torque surfaces across the evaluated controllers. Figure 9(a) depicts the classical μ-synthesis controller, which yields a smooth torque surface dedicated solely to robust tracking; because it lacks safety awareness, its control effort remains unaffected by obstacle proximity. In contrast, the cascaded μ-synthesis with CBF baseline in Fig. 9(b) exhibits localized regions with steep torque gradients once the barrier constraint activates. These sharp corrections preserve safety but introduce conservatism, chatter risk, and elevated control activity. Figure 9(c) presents the torque surface generated by the proposed DSA-μ framework. By incorporating the dynamic safety state into the safety-augmented generalized plant, the controller synthesizes tracking, robustness, and safety constraints simultaneously within the D–K iteration. Consequently, the resulting control surface adapts smoothly near the obstacle boundaries without localized torque spikes. The safety-driven surface profile in Fig. 9(d) further shows that control effort scales gradually as the safety distance $h(x)$ approaches zero, preventing the abrupt actuator saturation typical of post-hoc barrier filters while maintaining stability margins under parametric uncertainties.

Table II summarizes the safety performance of the evaluated controllers. Classical μ-synthesis violates the prescribed safety constraints, as indicated by the negative minimum barrier value ($h(x) = -0.0018$), since safety constraints are not incorporated during the controller synthesis stage. Incorporating a Control Barrier Function (CBF) as an online supervisory layer enables the cascaded μ–CBF architecture to eliminate collisions while preserving the forward invariance of the safe set. Consequently, the minimum barrier value remains positive ($h(x) = 0.0060$), indicating safe operation throughout the task.

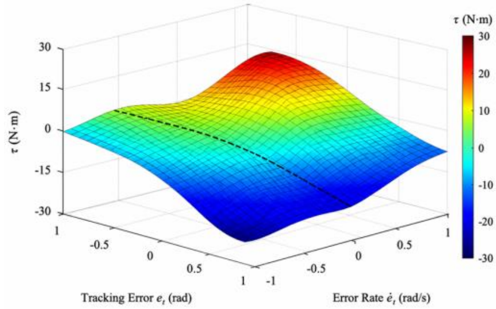

a) Conventional μ-synthesis controller

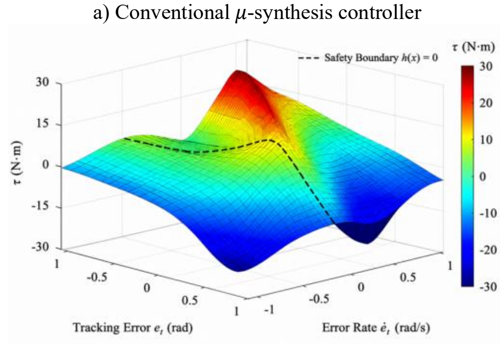

(b) Cascaded μ- CBF controller

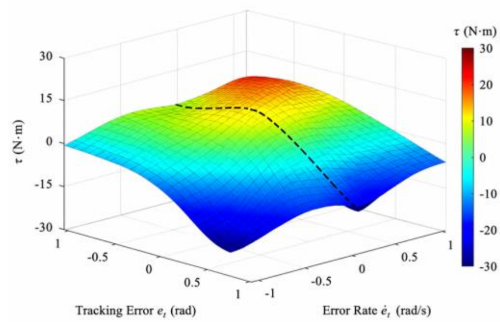

(c) Proposed DSA-μ controller

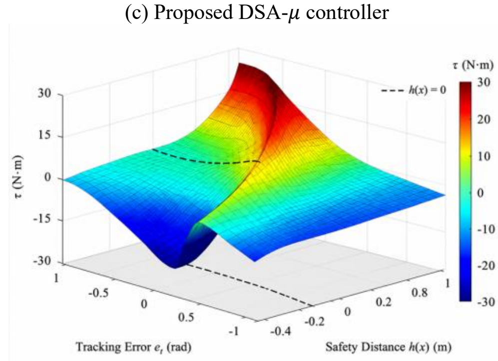

(d) Safety-induced Proposed DSA-μ controller

Fig. 9. Comparison of control torque surfaces generated by different strategies for the three-DOF robotic manipulator

However, because safety is enforced through a separate online quadratic programming (QP) filter, the controller operates closer to the safety boundary. In contrast, the proposed DSA-μ framework integrates the Dynamic Safety State directly into the Safety-Augmented Generalized Plant, allowing safety specifications to be incorporated during robust controller synthesis. As a result, the proposed controller achieves the highest minimum barrier value ($h(x) = 0.0152$) while satisfying all prescribed safety constraints, indicating a larger safety margin and improved robustness under structured uncertainties.

TABLE II Safety Performance Comparison

Controller	**Collision**	**Min $h(x)$**	**Safety Violation**
Classical μ	Yes	-0.0018	Violated
Cascaded μ–CBF	No	0.0060	Satisfied
Proposed DSA-μ	No	**0.0152**	Satisfied

Table III compares the robust stability margins across all evaluated controllers. Conventional μ-synthesis and cascaded μ-CBF reduce the upper bound below unity, whereas the proposed DSA-μ framework achieves the lowest overall peak upper bound ($\bar{\mu} = 0.63$), delivering the highest stability margin. These metrics confirm that formulating safety dynamics within the Safety-Augmented Generalized Plant directly enhances robust stability bounds without compromising tracking accuracy.

To further evaluate robustness, external disturbance torques are applied to all joints during $3 \le t \le 5$ s, $\tau_d = \begin{bmatrix} 5\sin(2t) \\ 4\cos(3t) \\ 3\sin(4t) \end{bmatrix}$ N · m, in addition to the structured parametric uncertainties. Figure 10 compares the transient tracking errors across all evaluated controllers under these composite stress conditions. While baseline $\mathcal{H}_\infty$ control improves disturbance attenuation, its tracking accuracy degrades under substantial parametric variations. Standard μ-synthesis preserves robust stability but exhibits pronounced transient spikes when nearing the obstacle boundary. Conversely, the casecaded μ-CBF and the proposed DSA-μ framework achieves the lowest peak tracking error. The proposed approach shows the fastest transient recovery, proving that unifying safety dynamics with robust synthesis inside the Safety-Augmented Generalized Plant enhances overall disturbance rejection without compromising safety constraints.

TABLE III Robust Stability Margin Comparison Under Structured Uncertainties

Controller	**$\Vert T_{zw} \Vert_\infty$**	**$\bar{\mu}$**	**Robust Stability**
Classical μ	1.19	0.82	Yes
Cascaded μ–CBF	0.96	0.74	Yes
Proposed DSA-μ	**0.74**	**0.63**	**Yes**

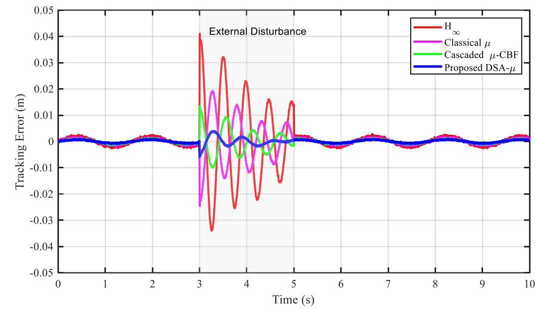

Fig. 10. Trajectory-tracking errors under structured parametric uncertainties and external disturbances.

Table IV compares the robustness of the evaluated controllers under structured parametric uncertainties and external disturbances. As expected, CTC exhibits the largest tracking errors and the highest performance degradation due to its reliance on the nominal model. The $\mathcal{H}_\infty$ controller improves disturbance rejection, while classical μ-synthesis further enhances robustness by explicitly accounting for structured uncertainties during controller synthesis. The cascaded μ–CBF architecture provides additional performance improvement by enforcing safety through an online barrier-based QP. However, the proposed DSA-μ framework achieves the highest level of safety performance among the evaluated controllers, yielding the lowest RMSE (0.008 m), the smallest maximum tracking error (0.018 m), the shortest settling time (0.61 s), and the lowest performance degradation (8.9%). These results demonstrate that jointly integrating safety and robustness within the Safety-Augmented Generalized Plant provides superior robustness compared with conventional cascaded architectures under structured uncertainties. It should be explained that although the CBF is introduced primarily to guarantee safety, its intervention also prevents the manipulator from entering operating regions where actuator saturation and joint-limit nonlinearities degrade closed-loop performance. Consequently, the observed reduction in tracking error is not a direct consequence of the CBF optimization itself but rather an indirect effect of maintaining the system within a region where the μ-synthesized controller effective. It should be noted that performance degradation is computed as the percentage increase in RMSE relative to the nominal (uncertainty-free) case.

Table V compares the proposed DSA-μ framework with recent safety-critical robotic controllers over 1,000 Monte Carlo simulation runs under structured parametric uncertainties and external disturbances. The proposed controller achieves the lowest trajectory-tracking RMSE of 0.0080 m (8.0 mm), representing a 35.2% reduction compared with the best-performing baseline method. In addition, it requires the shortest average computation time (0.68 ms) and achieves the highest task success rate (98.9%), demonstrating an effective balance between robustness, safety, and real-time computational efficiency. Although the proposed controller maintains a slightly smaller minimum clearance (8.0 cm) than the reference methods, it satisfies all prescribed safety constraints while exhibiting less conservative obstacle avoidance, thereby utilizing the available workspace more efficiently without compromising safety.

TABLE IV Robustness Performance Under Structured Uncertainty

Controller	**RMSE (m)**	**Max. Error (m)**	**Settling Time (s)**	**Performance Degradation (%)**	**Robust Stability**
Computed Torque Control (CTC)	0.062	0.128	1.84	52.3	No
MPC	0.0430	0.089	1.36	38.6	Marginal
$\mathcal{H}_\infty$	0.0340	0.071	1.21	31.4	Yes
Classical μ	0.0210	0.046	0.93	24.8	Yes
Cascaded μ–CBF	0.0123	0.026	0.76	18.9	Yes
Proposed DSA-μ	**0.0080**	**0.018**	**0.61**	8.9	**Yes**

TABLE V Comparison of the Proposed DSA-μ Framework with Recent Safety-Critical Robotic Controllers

Method	**RMSE**	**Min. Clearance**	**CPU Time**	**Success**
	(m)	(cm)	(ms)	(%)
Zhang et al. [17]	0.0260	8.5	0.81	95.5
McIlvanna et al. [18]	0.0180	8.6	0.78	94.8
Dai et al. [19]	0.0150	8.4	0.74	96.2
Li et al. [20]	0.0124	8.5	0.72	96.8
Proposed DSA-μ	**0.0080**	**8.0**	**0.68**	**98.9**

These improvements stem from integrating the Dynamic Safety State directly into the Safety-Augmented Generalized Plant, allowing robustness and safety to be addressed simultaneously during the D–K synthesis.

VI. Conclusion

This paper introduced the Dynamic Safety-Augmented μ-Synthesis ($\mathrm{DSA}-\mu$) framework to address the long-standing coupling between structured parametric uncertainties and strict state-space safety constraints in robotic manipulators. By embedding Control Barrier Function (CBF) dynamics directly into the generalized plant prior to synthesis, $\mathrm{DSA}-\mu$ achieves simultaneous optimization of robust performance and forward invariance within a single D–K iteration procedure. This unified formulation eliminates the structural vulnerabilities, control conflicts, and optimization infeasibilities inherent to post-hoc supervisory safety filters (such as cascaded CBF-QPs). Comparative simulation studies on a 3-DOF planar manipulator under structured inertial variations, actuator saturation, and dynamic obstacles confirmed the technical superiority of the proposed framework. Specifically, $\mathrm{DSA}-\mu$ strictly preserved set invariance while achieving a reduction in trajectory-tracking RMSE compared to conventional cascaded μ-CBF baselines. Furthermore, because the dynamic augmentation preserves the standard LFT structure, the architecture integrates seamlessly into existing robust control toolboxes without requiring secondary real-time optimization solvers. Future research will extend this framework to experimental physical testbeds, and real-time adaptive uncertainty estimation.

References

[1] B. Siciliano and O. Khatib, Eds., *Springer Handbook of Robotics*, 2nd ed. Springer, 2016.

[2] F. Sabahi, "Robot Action Space of Tractable Subsumption Architecture" *International Journal of Industrial Electronics Control and Optimization*, vol. 2, no. 4, pp. 297-304, 2019.

[3] V. Mihaly, M. Șușcă, and P. Dobra, "Fixed-structure robust feedback linearization for full relative degree nonlinear systems," IEEE/CAA J. Autom. Sinica, vol. 12, no. 10, pp. 2026–2039, 2025.

[4] A. Packard and J. Doyle, "The Complex Structured Singular Value," *Automatica*, vol. 29, no. 1, pp. 71–109, 1993.

[5] A. D. Ames, S. Coogan, M. Egerstedt, G. Notomista, K. Sreenath, and P. Tabuada, "Control Barrier Functions: Theory and Applications," in *Proc. European Control Conference (ECC)*, 2019, pp. 3420–3431.

[6] A. D. Ames, X. Xu, J. W. Grizzle, and P. Tabuada, "Control Barrier Function Based Quadratic Programs for Safety Critical Systems," *IEEE Transactions on Automatic Control*, vol. 62, no. 8, pp. 3861–3876, 2017.

[7] K. Garg, J. Usevitch, J. Breeden, M. Black, D. Agrawal, H. Parwana, and D. Panagou, "Advances in the Theory of Control Barrier Functions: Addressing Practical Challenges in Safe Control Synthesis for Autonomous and Robotic Systems," *Annual Reviews in Control*, vol. 57, Art. no. 100945, 2024.

[8] W. Xiao and C. Belta, "High-Order Control Barrier Functions," *IEEE Transactions on Automatic Control*, vol. 67, no. 7, pp. 3655–3662, 2022.

[9] W. S. Cortez, D. V. Dimarogonas, and M. Egerstedt, "Control Barrier Functions for Mechanical Systems:

Theory and Robotic Applications," *IEEE Control Systems Letters*, vol. 5, no. 6, pp. 1955–1960, 2021.

[10] R. K. Cosner, A. J. Taylor, and A. D. Ames, "Measurement-Robust Control Barrier Functions: Certainty Equivalence Under State Estimation Uncertainty," *IEEE Control Systems Letters*, vol. 5, no. 6, pp. 1959–1964, 2021.

[11] S. Kang, Y. Chen, H. Yang, and M. Pavone, "Verification and Synthesis of Robust Control Barrier Functions: Multilevel Polynomial Optimization and Semidefinite Relaxation," in *Proc. IEEE 62nd Conference on Decision and Control (CDC)*, Singapore, 2023, pp. 6082–6089.

[12] H. Wang, J. Peng, . Liu, W. He, Y. Wang "Adaptive Safety-Based Tracking Control for Uncertain Robotic Systems With Input-Output Constraints: A Neural Network-Based Augmented High-Order Control Barrier Function Approach," IEEE Transactions on Cybernetics, vol. 55, no. 9, pp.4453-4465, 2025.

[13] S. Skogestad and I. Postlethwaite, *Multivariable Feedback Control: Analysis and Design*, 2nd ed. Wiley, 2005.

[14] M. Karkoub and G. J. Balas, "Robust Control of Flexible Manipulators via μ-Synthesis," *Control Engineering Practice*, vol. 8, no. 7, pp. 725–734, 2000.

[15] Don Riley, Matlab and Simulink, Copyright (c) 2001.

[16] F. Sabahi, "Data-Driven μ-Robust Control with CBF-Based Safety for Robotic Manipulators " 34th Annual International Conference of Iranian Society of Mechanical Engineers, ISME2026, Hamedan, May 2026, pp.1-6.

[17] S. Zhang, D.-H. Zhai, Y. Xiong, J. Lin, and Y. Xia, "Safety-Critical Control for Robotic Systems With Uncertain Model via Control Barrier Function," *International Journal of Robust and Nonlinear Control*, vol. 33, no. 6, pp. 3661–3676, Apr. 2023.

[18] S. McIlvanna, M. Van, Y. Sun, N. N. Minh, and W. Naeem, "Parameter Prediction of Control Barrier Function Parameters for Robotic Manipulator Obstacle Avoidance," in *Proc. IECON 2023–49th Annual Conference of the IEEE Industrial Electronics Society*, Singapore, 2023, pp. 1–6.

[19] B. Dai, R. Khorrambakht, P. Krishnamurthy, V. Goncalves, A. Tzes, and F. Khorrami, "Safe Navigation and Obstacle Avoidance Using Differentiable Optimization-Based Control Barrier Functions," *IEEE Robotics and Automation Letters*, vol. 8, no. 9, pp. 5376–5383, 2023.

[20] C. Li, Z. Zhang, N. Ahmed, Q. Liu, F. Liu, and M. Buss, "Safe Feedback Motion Planning in Unknown Environments: An Instantaneous Local Control Barrier Function Approach," *Journal of Intelligent & Robotic Systems*, vol. 109, Art. no. 40, 2023.

Farnaz Sabahi received the Ph.D. degree in control engineering from the Department of Electrical Engineering, Ferdowsi University of Mashhad, Mashhad, Iran. She is currently Associate Professor and the director of S-answer laboratory with Department of Electrical Engineering, Faculty of Electrical and Computer Engineering, Urmia University, Urmia, Iran. Her current research interests include the areas of decision systems, robust control, robotics, fuzzy theory and machine learning.